NANO LETTERS

2007
Vol. 7, No. 12
3675−3680

High-Order Waveguide Modes in ZnO Nanowires

Tobias Voss,* Geoffry T. Svacha, and Eric Mazur*

Department of Physics and School of Engineering and Applied Sciences, Harvard University, 9 Oxford Street, Cambridge, Massachusetts 02138

Sven Müller and Carsten Ronning

II. Physikalisches Institut, University of Göttingen, Göttingen, Germany

Denan Konjhodzic and Frank Marlow

Max-Planck-Institut für Kohlenforschung, Mülheim, Germany

Received August 7, 2007; Revised Manuscript Received October 5, 2007

ABSTRACT

We use tapered silica fibers to inject laser light into ZnO nanowires with diameters around 250 nm to study their waveguiding properties. We find that high-order waveguide modes are frequently excited and carry significant intensity at the wire surface. Numerical simulations reproduce the experimental observations and indicate a coupling efficiency between silica and ZnO nanowires of 50%. Experimentally, we find an emission angle from the ZnO nanowires of about 90°, which is in agreement with the simulations.

The investigation of the structural, electrical, and optical properties of semiconductor nanowires has been an active field of research for the past couple of years because these nanowires afford a large variety of novel nanoscale electronic and optoelectronic devices like piezoelectric nanogenerators,[1] field effect transistors,[2] light-emitting diodes,[3,4] lasers[5,6] and waveguides.[5−9] These applications are feasible because the high crystalline quality, low defect density, smooth sidewalls, and well-defined end facets of the nanowires make them suitable as waveguides and resonators for optical modes in the visible or near-IR spectrum. In particular, nanowires made of the large band gap wurtzite II−VI semiconductor zinc oxide (ZnO) have been extensively investigated, because this material system is a promising candidate for the fabrication of nanoscale light emitters in the near-UV spectral region.[10−12] Furthermore, ZnO is an easy to handle, nontoxic material possessing a large exciton binding energy (60 meV),[9] which allows efficient excitonic light-emission processes even at room temperature. ZnO nanowires can be grown in large quantities in a well-defined diameter range up to lengths of several tens of micrometers in high-temperature vapor−liquid−solid growth processes, sometimes with gold as the catalyst.

To couple light into the semiconductor nanowires, we use silica nanowires.[13] Silica nanowires and tapered fibers have attracted considerable interest in the past few years, because they can be fabricated by taper drawing from standard silica optical fibers[13] with lengths of up to several tens of millimeters and a surprisingly high diameter uniformity. External laser light can be easily coupled into the silica nanowires through the macroscopic optical fiber to which the nanowires are still attached.

In this Letter, we show that the combination of silica nanowires, which are fabricated in a top-down approach, and ZnO nanowires, obtained from a bottom-up growth process, allows a detailed experimental investigation of the passive waveguiding properties of the semiconductor nanowires. By carrying out numerical finite-difference time-domain simulations, we find that it is possible to achieve a high coupling efficiency from the tapered silica fibers into ZnO. We study the evanescent field of ZnO nanowires as a function of their diameter and analyze the condition for single-mode and multimode waveguiding. In both the experiments and simulations, we find that for typical ZnO nanowire diameters of about 250 nm and laser light in the visible spectral region the coupling from silica to ZnO nanowires frequently leads to the excitation of high-order waveguide modes. We also use our combination of silica and ZnO nanowires to study the emission of low-order waveguide modes from the end facets of the ZnO nanowires and compare the results with our simulations.

We synthesized single crystalline zinc oxide (ZnO) nanowires in a horizontal tube furnace by a vapor transport

* To whom correspondence should be addressed.

10.1021/nl071958w CCC: $37.00
Published on Web 11/17/2007

technique.[14] High-purity ZnO powder as source material was placed in an alumina boat and heated up to 1620 K allowing evaporation. Silicon substrates covered with a 4 nm thin Au film were placed at the cooler end of the tube furnace at a temperature of around 1370 K. The vapor was transported at a pressure of 100 mbar by Ar gas flow of 50 sccm to the substrates initiating the catalytic driven vapor−liquid−solid (VLS) growth process[15] of the ZnO nanowires. The as-deposited nanowires are typically up to 100 μm long and between 40 and 500 nm in diameter, as determined by scanning electron microscopy (SEM). Energy-dispersive spectrometry reveals only stoichiometric zinc and oxygen signals; transmission electron microscopy and X-ray diffraction confirm that the nanowires are of wurtzite structure and the *c*-axis is in the growth direction.

We mechanically disperse 20−80 μm long ZnO nanowires onto thin glass substrates coated with a 80 nm thick mesoporous silica film.[16,17] The mesoporous films have monodisperse, 8 nm wide pores and are deposited using a dip-coating process. The resulting films have a refractive index of about $n = 1.185$ throughout the visible spectral region,[16] preventing parasitic coupling into the substrates. Combined with their extremely high homogeneity and flatness, these layers also help minimize losses and noise due to scattering at the output sides of the silica and ZnO nanowires, which is crucial when investigating coupling and waveguiding processes. Because the refractive index of mesoporous silica is much lower than that of both the silica and ZnO nanowires, we can treat the nanowires as freestanding, air-clad waveguides in our numerical simulations.

Silica nanowires were fabricated with a conventional fiber-tapering technique[18] to produce low-loss submicrometer diameter wires that remain attached to a standard fiber on one side. The fiber-pulling setup consists of a regulated hydrogen torch and two computer-controlled linear stages. The parameters for the fiber-pulling system, such as speed, acceleration, fiber tension, and position of the flame, were optimized to yield low-loss taper regions.

To study the coupling and waveguiding properties of the ZnO nanowires, we launched continuous wave laser light ($\lambda = 532$ nm, $P = 1$ mW) into a silica optical fiber mounted on a micropositioning stage. We used either the as-fabricated silica nanowires or cut them off close to the tapered region, using the end of the tapered region to couple light into the ZnO nanowires. We observed the coupling using an inverted microscope with a 100× oil-immersion objective (numerical aperture 1.4) and used the micropositioning stage to bring the end of the silica fiber near an individual ZnO nanowire.

Figure 1 shows the coupling of green laser light from the tapered silica fiber into a ZnO nanowire. We observe no coupling between the two waveguides at all (Figure 1a) until the distance between them is smaller than about 1 μm and light is seen exiting the end facet (Figure 1b). Figure 1c shows the emission of light from a growth imperfection along the length of the nanowire. In Figure 1d, we show that light also couples efficiently between two ZnO nanowires lying on top of each other.

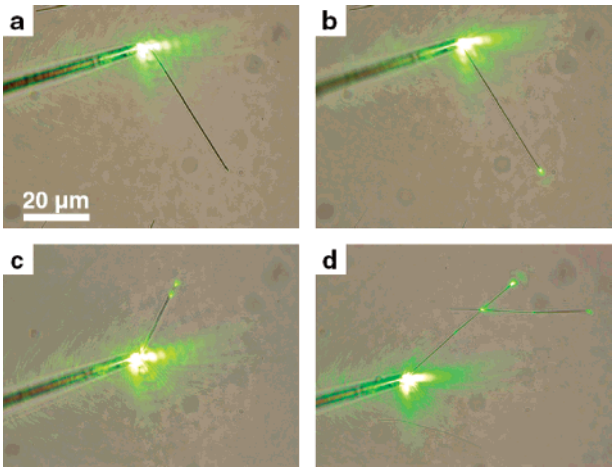

Figure 1. Waveguiding in single ZnO nanowires. (a) Tapered silica fiber close to the nanowire but no coupling. (b) Coupling of light into a low-order waveguide mode of the ZnO nanowire. (c) Nanowire with imperfections leading to additional losses and two output points. (d) Coupling between two ZnO nanowires lying on top of each other.

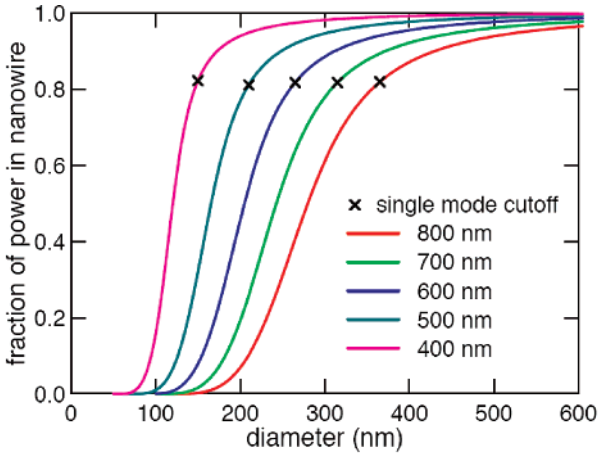

Figure 2. Diameter and wavelength dependence of the fraction of power guided in the lowest order HE_{11} mode inside a cylindrical ZnO nanowire. The remaining part of the power is guided in the evanescent field. The crosses show the transition between the single-mode and multimode waveguiding regimes (single-mode guiding occurs for diameters smaller than that at the cross).

To understand the relevant properties and mechanisms that govern the waveguiding and coupling observed in Figure 1, we performed numerical simulations of the mode distribution in the visible part of the spectrum, where ZnO is completely transparent. We started with an analytically solvable model[20] treating the ZnO nanowire as a perfect cylinder, neglecting its hexagonal structure. The simulations include the dispersion of ZnO by approximating the refractive index with a Sellmeier type equation.[19] In Figure 2, we show the wire diameter and wavelength dependence of the calculated power of the lowest-order HE_{11} mode that is carried inside the cylindrical ZnO nanowire. The crosses mark the transition from single-mode to multimode waveguiding obtained from the condition[20] for single-mode waveguiding: $2\pi d/\lambda_0 \, (n_1^2 - n_{air}^2)^{1/2} < 2.405$, where d is the wire diameter, λ_0 is the vacuum wavelength, and n_1 and n_{air} are the refractive indices

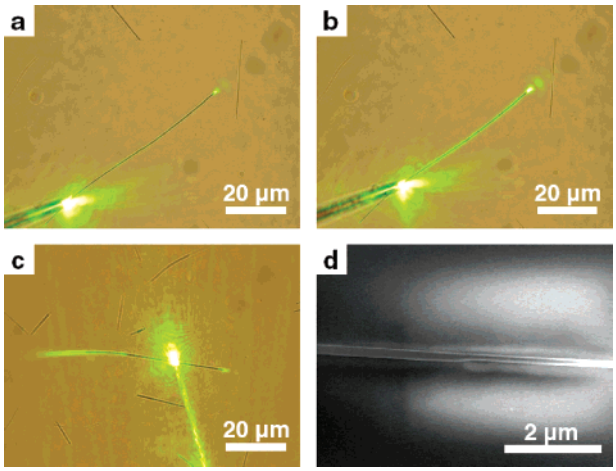

Figure 3. Experimental observation multimode waveguiding. Top row: a slight change in the alignment of the silica nanowire changes the mode excited in the ZnO nanowire from (a) a low-order to (b) a high-order mode with a significant intensity guided at the surface. Scattering at the high-quality substrates leads to low losses of this mode, which make this mode visible under the microscope. (c) High-order mode can also be excited when the diameter of the nanowire changes. (d) SEM picture showing the diameter change that causes the excitation of the higher-order modes in panel c.

of ZnO and air, respectively. The transition occurs when the power guided in the ZnO nanowires is less than about 80%. The critical diameter for single-mode waveguiding is in the range between $d = 350$ nm ($\lambda = 800$ nm) and $d = 150$ nm ($\lambda = 400$ nm). Figure 2 shows that the fraction of power guided inside the nanowire sharply decreases below the critical diameter, especially at short wavelengths. The results in Figure 2 agree with previous results obtained for silica and silicon nanowires.[20] Because the diameter of the ZnO nanowires is about 250 nm, we can expect higher-order waveguiding for wavelengths below 600 nm.

Figure 3a,b shows that a slight change in the alignment of the silica-tapered fiber with respect to the ZnO nanowire dramatically changes the coupling and waveguiding conditions. In Figure 3a, the coupling, guiding, and emission of the waveguide mode is the same as in Figure 1b, but a small adjustment of the tapered fiber leads to the excitation of high-order waveguide modes (Figure 3b). These high-order modes carry a significant additional fraction of power at the nanowire surface and even outside the nanowire as evanescent fields. This can be seen by comparing the emitted intensities at the nanowire ends in Figure 3a,b.

High-order modes can also be generated at imperfections along the ZnO nanowire. Figure 3c shows a transition from single-mode to multimode waveguiding along a nanowire. An SEM picture of that nanowire shows that the diameter of the nanowire increases at the transition point (Figure 3d). We observed many nanowires that exhibited a similar single- to multimode transition.

An enlarged view of the end of the nanowire in Figure 3a shows the emission profile (Figure 4a). The dashed white lines show that the emission angle is about 90°. Figure 4b shows a two-dimensional finite-difference time domain (FDTD) simulation[21] of the emission of a single-mode pulse

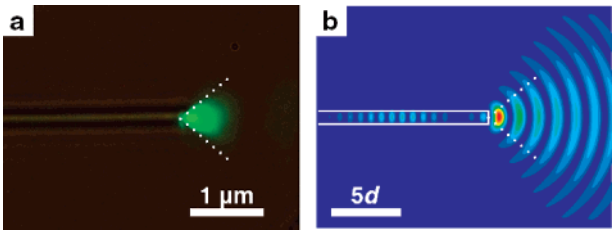

Figure 4. (a) Magnified view of the conical emission of a low-order guided mode from a ZnO nanowire. The emission angle is approximately 90° (dotted lines). (b) FDTD calculation of the square of the electric field of a light pulse emitted from a nanowire of diameter d.

from a ZnO nanowire using a constant index of refraction ($n = 2$). We plot the square of the electric field in z-direction (perpendicular to the plane of the figure) after the pulse has been emitted from the right end of the nanowire. A small fraction of the light has been reflected and travels back to the left inside the nanowire. The lateral dimensions are given in units of the ZnO nanowire diameter d_{ZnO} and the wavelength has been chosen to be $2.66d_{ZnO}$, which corresponds to the situation in Figure 4a ($\lambda = 532$ nm and $d = 200$ nm). The simulation confirms our experimental observation of directed emission from the nanowire waveguide mode into a cone with an angle of about 90° as indicated by the dotted white lines in Figure 4a.

As our results in Figure 2 and 3 demonstrate, ZnO nanowires with diameters around 200 nm can serve as multimode waveguides for visible light. To determine the maximum achievable coupling efficiency and to understand the origin and properties of the high-order waveguide modes, we numerically simulated the waveguiding and coupling between silica and ZnO nanowires using the FDTD technique.[21] The results of the FDTD simulations are scalable if the wavelength and the lateral dimensions of the nanowires are multiplied by the same number, and as long as the refractive indices of the involved materials are constant. For the simulations presented here, we assume constant refractive indices of $n_{ZnO} = 2$, $n_{silica} = 1.46$, and $n_{air} = 1$, which is a good approximation for the wavelength range between 400 and 1000 nm. In all simulations, the vector of the electric field is perpendicular to the plane of the nanowires. We simulated the propagation of a pulse from a silica to a ZnO nanowire in two dimensions for various angles between the symmetry axes of the two nanowires, as shown in the inset in Figure 5a. A light pulse uniformly illuminates the left end of the silica fiber, exciting a low-order mode that travels to the right. At the interface between the silica and the ZnO nanowire, part of the pulse is reflected, a second part is scattered, and a third part is coupled into the waveguide modes of the ZnO nanowire.

To estimate the coupling efficiency, we calculated the transmission into the ZnO nanowire by dividing the integrated power in the ZnO nanowire by the integrated power coupled into the silica nanowire. Figure 5a shows how this transmission depends on the angle between the nanowires for nanowires of diameters $d_{silica} = 4d_{ZnO}$ and letting the central wavelength (measured in vacuum) of the light pulse

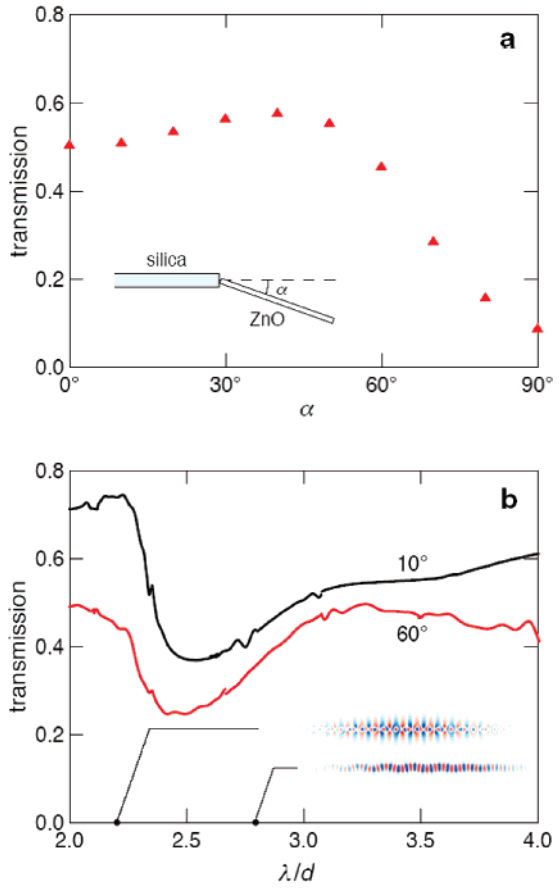

Figure 5. Coupling efficiency between a silica fiber with 1 μm diameter and a ZnO nanowire with 250 nm obtained from numerical FDTD simulations. (a) Transmission as a function of the angle between the silica fiber and the ZnO nanowire. The inset shows the geometry used in the simulation. (b) Transmission as a function of the wavelength for two different coupling angles. The inset shows the electric field profiles in the ZnO nanowire at $\lambda/d = 2.2$ and 2.8.

be three times the diameter of the ZnO nanowire, so that $\lambda = 600$ nm, $d_{ZnO} = 200$ nm, and $d_{silica} = 800$ nm, in accordance with our experimental conditions. The simulations show that the coupling efficiency exceeds 0.50 for angles up to 50°. For angles larger than 50°, the transmission decreases substantially, but remains above 0.10 even when the nanowires are perpendicular to each other. Varying the wavelength between $2d_{ZnO}$ and $4d_{ZnO}$ (not shown here) changes the transmission by less than 0.1. Likewise, we find that the transmission depends weakly (<0.1) on the diameter ratio for the range $2 < d_{silica}/d_{ZnO} < 4$. Introducing a small gap between the two nanowires (gap length $\leq \lambda/5$) decreases the transmission by only a few percent.

Figure 5b shows the wavelength dependence of the transmission for two nanowire angles of 10 and 60°. The wavelength scale covers the range from $2d_{ZnO}$ to $4d_{ZnO}$ which corresponds to 400 nm $< \lambda <$ 800 nm for our experimental condition ($d_{ZnO} = 200$ nm). For both angles, the transmission spectra show the same general wavelength dependence. The main difference between the two angles is that the transmission at 60° is about 0.10−0.25 smaller. This difference is in line with the results presented in Figure 5a. The transmission spectra show that the coupling efficiency decreases as we decrease the wavelength from a value of $4d_{ZnO}$; the simulations show that this decrease is due to increased scattering at the interface between the nanowires. Below a wavelength of $2.5d_{ZnO}$, the transmission increases sharply for both angles. At an angle of 10°, the transmission exceeds 0.7, significantly higher than at longer wavelengths.

The inset in Figure 5b shows the mode profiles of the transmitted pulse at wavelengths of $2.2d_{ZnO}$ and $2.8d_{ZnO}$. The blue and the red correspond to maximum negative and positive amplitudes of the electric field, respectively. The profile for the long-wavelength pulse shows a low-order mode with a noticeable zigzag-like propagation through the ZnO nanowire. The profile for the short-wavelength pulse shows additional high-order mode components with strong field amplitudes at the nanowire surface and significant evanescent-field amplitudes.

Although the photoluminescence properties of semiconductor nanowires have been studied experimentally,[10,11,22,23] their waveguiding properties remain largely unexplored. One reason is the lack of a robust, efficient, and well-understood optical technique to study individual nanowires. Figure 1 shows that silica-tapered fibers and silica nanowires are convenient, robust, and efficient tools to controllably inject light into the waveguide modes of individual semiconductor nanowires. Figure 1a,b shows that a considerable amount of light can be coupled into ZnO nanowires even when the angle between the two waveguides is large. Our technique thus permits the convenient and systematic study of the waveguiding properties of semiconductor nanowires. The technique can also be used to scan nanowires for potential imperfections and sources of additional loss (as shown in Figure 1c) before they are further processed into devices. The simple two-nanowire system in Figure 1d shows that silica-tapered fibers can be used to characterize the performance and loss of more complex optical nanowire circuits.

The low-index and low-loss mesoporous silica substrates prevent parasitic scattering from overshadowing the waveguiding characteristics. Because no light is emitted or scattered from any other part but the nanowire's end facet (Figure 1b), we can conclude that no significant losses occur during the waveguiding of low-order modes in the ZnO nanowire. The large index contrast between the waveguide materials and the mesoporous silica allows us to directly compare experimental results with simulations of air-clad waveguides.

The index of refraction n of semiconductor nanowires typically ranges between 2 and 4, and so the wavelength λ_{air}/n in these materials is substantially reduced. Consequently, the critical diameter for single mode waveguiding is distinctly smaller than for silica nanowires. Conversely, for a nanowire of fixed diameter, the limit for single-mode waveguiding is farther into the blue spectral region than for silica nanowires. Figure 2 shows that at the single-mode cutoff for ZnO ($n = 2$), 80% of the mode energy is confined in a small spatial region with a diameter between 150 and 350 nm, which is precisely the range of diameters for VLS-grown ZnO nanowires. The strong confinement is very desirable for efficient and low-loss waveguiding and wiring of light at the nanoscale.

The large index contrast between the ZnO and silica nanowires causes the excitation of high-order modes with substantial evanescent field contributions in the ZnO nanowires even for nanowires with diameters just slightly exceeding the single mode limit. These evanescent fields scatter at the surface of the nanowire as the high-order mode propagates along the nanowire waveguide, leading to the green appearance in Figure 3b. The high-order modes shown in Figure 3b propagate along the nanowire waveguide without intrinsic losses and are therefore distinctly different from whispering gallery modes that have been previously reported in ZnO nano- and microrods.[24]

Both the experimental results in Figure 3a,b and the simulations in Figure 5b show that the excitation of high-order modes is controlled by the alignment between the nanowires. Depending on the application, either low- or high-order modes may be preferable. For example, the strong confiment provided by low-order modes enables low-loss nanoscale waveguiding. Likewise, low-order modes would maximize the overlap between the optical field and the semiconductor material in semiconductor amplifiers. On the other hand, high-order modes could be used to achieve efficient evanescent sensing and enhance coupling efficiency, as demonstrated in Figure 3a,b.

Our experiments show that the acceptance angle for launching waves into ZnO nanowires is large. Because the propagation of light is reversible, the acceptance and emission angles should be the same. Indeed, the emission cone angle of the nanowires is approximately 90°, as shown in Figure 4. While this angle is large, the emission is still clearly directed and the nanowire ends cannot be considered point sources, as previously reported for actively emitting short ZnO nanowires.[25]

The FDTD simulations presented in Figure 5 confirm the high coupling efficiency between the waveguide modes in the silica fibers and ZnO nanowires. Although the experimentally achievable efficiency might still be significantly below the theoretical value of 0.50, the simulations show that the efficiency is rather insensitive to the precise alignment for angles less than 50°. This maximum angle of 50° is in excellent agreement with the experimental observation of a 90° cone angle for emission in Figure 4. Within experimental accuracy, this cone angle is approximately twice the angle at which the coupling efficiency starts to decrease, as theoretically expected. The simulations show that the main physical parameter that determines the coupling efficiency is the large index contrast between both waveguide materials. All these results remain qualitatively the same if we rotate the linear polarization of the electric field from perpendicular to the plane of the nanowires to in-plane. While the absolute values of the transmission differ for the two polarization states, the excitation of high-order modes at shorter wavelengths occurs for both polarizations.

Figure 5b shows that for wavelengths above $2.5d_{ZnO}$ the transmission increases with increasing wavelength. The profiles of the electric field obtained in the simulations reveal that as the wavelength increases, scattering at the interface between the two wires decreases, increasing the amount of light that is coupled to the ZnO nanowire. For all angles studied, the transmission reaches a minimum at wavelengths around $2.5d_{ZnO}$. Below this wavelength the transmission is significantly higher. As the mode profiles in the inset of Figure 5b show, this increase coincides with the excitation of high-order modes during the coupling from the silica to the ZnO nanowire.

In summary, we used silica nanowires and tapered fibers to efficiently and controllably inject laser light into individual ZnO nanowires and study their waveguiding properties. The ZnO nanowires are placed on glass substrates covered with a layer of low-index mesoporous silica to prevent coupling of light from the silica-tapered fibers into the glass substrate and achieve very low parasitic scattering at the nanowire output facets. Finite difference time domain simulations reveal the dependence of the coupling efficiency from the silica into the ZnO nanowires on the angle between them and on the wavelength of the guided modes. The maximum efficiency can theoretically reach 50%. We showed that high-order waveguide modes with high intensities at the nanowire surface are frequently excited when light is coupled between nanowire waveguides with different refractive indices. We studied the single- and multimode waveguiding conditions for ZnO nanowires in numerical simulations and calculated the evanescent field strength of the lowest order mode of a cylindrical ZnO nanowire. We analyzed the emission of waveguide modes from ZnO nanowires and found a typical emission angle of 90° both experimentally and in the simulations for nanowires with diameters of about 200 nm. The wavelength dependence of the transmission efficiency and the behavior of high-order modes presented here facilitate the interpretation of semiconductor nanowire experiments and the optimization of semiconductor nanowire devices.

Acknowledgment. Several people contributed to the work described in this paper. T.V. conceived the basic idea for this work, designed the experiment, carried out the experiments, and performed the FDTD simulations. G.T.S. fabricated the silica-tapered fibers. C.R. and S.M. fabricated and characterized the ZnO nanowires. D.K. and F.M. fabricated and characterized the mesoporous silica substrates. E.M. supervised the research and contributed to the development of the manuscript. T.V. wrote the first draft of the manuscript; all authors subsequently took part in the revision process. T. Shih and M. T. Winkler provided feedback on the manuscript throughout its development. T.V., C.R., and S.M. acknowledge funding by the German Research Foundation through the Grants VO1265/3, VO1265/4-1, and Ro1198/7-1,2. The research described in this paper is also supported by the National Science Foundation under Contracts PHY-0117795 and ECS-0601520. The authors would also like to acknowledge the use of facilities of the Center for Nanoscale Systems, which is supported by the National Science Foundation's National Nanotechnology Infrastructure Network.

References

(1) Wang, Z. L.; Song, J. *Science* **2006**, *312*, 242.
(2) Li, Y.; Qian, F.; Xiang, J.; Lieber, C. M. *Mater. Today* **2006**, *9*, 18.
(3) Huang, Y.; Duan, X.; Lieber, C. M. *Small* **2005**, *1*, 142.

(4) Bao, J.; Zimmler, M. A.; Capasso, F. *Nanoletters* **2006**, *6*, 1719.
(5) Pauzauskie, P. J.; Yang, P. *Mater. Today* **2006**, *9*, 36.
(6) Hauschild, R.; Kalt, H. *Appl. Phys. Lett.* **2006**, *89*, 123107.
(7) Law, M.; Sirbuly, D. J.; Johnson, J. C.; Goldberger, J.; Saykally, R. J.; Yang, P. *Science* **2004**, *305*, 1269.
(8) Ye, Z.; Hu, X.; Li, M.; Ho, K.-M.; Yang, P. *Appl. Phys. Lett.* **2006**, *89*, 241108.
(9) Maslov, A. V.; Ning, C. Z. *Appl. Phys. Lett.* **2003**, *83*, 1237.
(10) Look, D. C. *Mater. Sci. Eng.* **2001**, *B80*, 383.
(11) Voss, T.; Bekeny, C.; Wischmeier, L.; Gafsi, H.; Börner, S.; Schade, W.; Mofor, A. C.; Bakin, A.; Waag, A. *Appl. Phys. Lett.* **2006**, *89*, 182107.
(12) Wischmeier, L.; Voss, T.; Börner, S.; Schade, W. *Appl. Phys. A* **2006**, *84*, 111.
(13) Tong, L.; Gattass, R. R.; Ashcom, J. B.; He, S.; Lou, J.; Shen, M.; Maxwell, I.; Mazur, E. *Nature* **2003**, *426*, 816.
(14) Borchers, C.; Müller, S.; Stichtenoth, D.; Schwen, D.; Ronning, C. *J. Phys. Chem. B* **2006**, *110*, 1656.
(15) Wagner, R. S.; Ellis, W. C. *Appl. Phys. Lett.* **1964**, *4*, 89.
(16) Konjhodzic, D.; Bretinger, H.; Wilczok, U.; Dreier, A.; Ladenburger, A.; Schmidt, M.; Eich, M.; Marlow, F. *Appl. Phys. A* **2005**, *81*, 425.
(17) Schmidt, M.; Boettger, G.; Eich, M.; Morgenroth, W.; Huebner, U.; Meyer, H. G.; Konjhodzic, D.; Bretinger, H.; Marlow, F. *Appl. Phys. Lett.* **2004**, *85*, 16.
(18) Gattass, R.; Svacha, G.; Tong, L.; Mazur, E. *Opt. Exp.* **2006**, *14*, 9408.
(19) Yoshikawa, H.; Adachi, S. *Jpn. J. Appl. Phys.* **1997**, *36*, 6237.
(20) Tong, L.; Lou, J.; Mazur, E. *Opt. Exp.* **2004**, *12*, 1025.
(21) Farjadpour, A.; Roundy, D.; Rodriguez, A.; Ibanescu, M.; Bermel, P.; Joannopoulos, J. D.; Johnson, S. G.; Burr, G. *Opt. Lett.* **2006**, *31*, 2972.
(22) Zhao, Q. X.; Willander, M.; Morjan, R. E.; Hu, Q.-H.; Campbell, E. E. B. *Appl. Phys. Lett.* **2003**, *83*, 165.
(23) Yi, G.-C.; Wang, C.; Park, W. I. *Semicond. Sci. Technol.* **2005**, *20*, S22.
(24) Nobis, T.; Kaidashev, E.; Rahm, A.; Lorenz, M.; Grundmann, M. *Phys. Rev. Lett.* **2004**, *93*, 103903.
(25) Vugt, L. K.; van Rühle, S.; Vanmaekelbergh, D. *Nanoletters* **2006**, *6*, 2707.

NL071958W